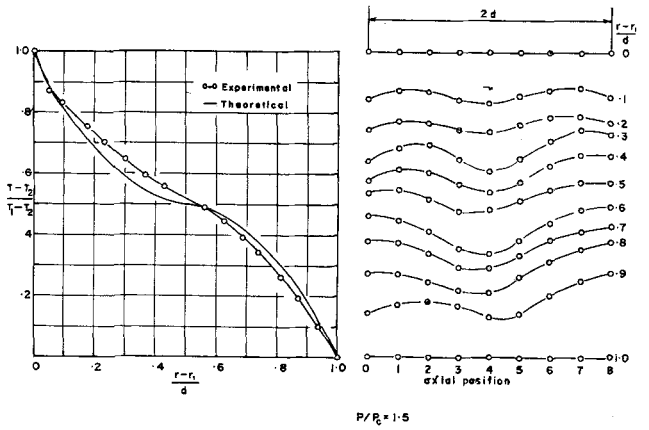

Fig. 4a. Radial and axial temperature profiles.

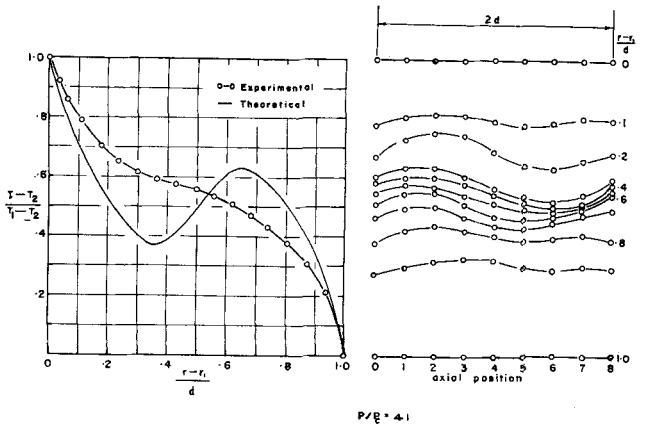

Fig. 4b. Radial and axial temperature profiles.

One has the rate of heat transfer from Equation (29). The Nusselt number is given by

$$N_{Nu} = \frac{2hd}{k} = 2\left[1 + 1.4472\left(1 - \frac{1{,}708}{N_{Ta^*}}\right)\right] \quad (32)$$

and

$$\frac{N_{Nu}}{N_{Nuk}} = 1 + 1.4472\left(1 - \frac{1{,}708}{N_{Ta^*}}\right) \quad (33)$$

Since the Prandtl number for air is close to unity (that is $N_{Pr} = 0.7$), the above theoretical analysis may be applied. Figure 3 shows the comparison of theoretical analysis to the experimental results of air, and it can be seen that the agreement is satisfactory.

DISCUSSION AND CONCLUSION

Figure 3 shows that the theoretical analysis for air gives a reasonably correct result for the heat transfer for a short range of Taylor numbers above the critical value. It is believed that the gradual divergence between theoretical and experimental values as the Taylor number increases is due to the increasing divergence from reality of the simplifying assumption made in the derivation; that is velocity and temperature distributions become increasingly different in fact from those assumed in the theory as the Taylor number increases.

Thus Figure 4a shows the temperature profiles as measured and as predicted theoretically for a relatively low Taylor number. The differences observed are relatively small and are probably due as much to the difficulties of accurate temperature measurements in the fluid as to theoretical errors. On the other hand Figure 4b shows that the measured and theoretically predicted profiles are completely different for a high Taylor number. The reversal of sign of the temperature gradient in the central region of the theoretically predicted profile is clearly not realistic, and the theory fails.

Presented along with the radial temperature profiles in Figure 4 are axial temperature profiles. The periodic variation of temperature in an axial direction can easily be seen; this would indicate that the temperature within the vortex is nearly constant axially but with some sinusoidal disturbance.

In Part II the analysis for substances with $N_{Pr} = 1$ will be extended to include a higher range of Taylor numbers. In addition the heat transfer characteristics of fluids with Prandtl numbers different from 1 will also be investigated.

LITERATURE CITED

1. Bjorklund, I. S., and W. M. Kays, *Am. Soc. Mech. Engrs. Heat Transfer Journal*, **81**, 175 (1959).
2. Chandrasekhar, S., *Proc. Roy. Soc.*, **A216**, 293 (1953).
3. Haas, F. C., and A. H. Nissan, *Proc. Roy. Soc.*, **A261**, 215 (1961).
4. ————, International Heat Transfer Conference, Boulder, Colorado, Vol. 3, p. 643 (1961).
5. Stuart, J. T., *Fluid Mechanics*, 4, 1 (1958).
6. Tachibana, F., S. Fukui, and H. Mitsumura, *Jap. Soc. Mech. Engrs.*, 3, 9, 119 (1960).
7. Taylor, G. I., *Phil. Trans.*, **A223**, 289 (1923).
8. Becker, K. M., and J. Kaye, *Trans. Am. Soc. Mech. Engrs.*, 84, Series C, No. 2 (1962).

Part II. $N_{Pr} \neq 1$

In Part I a review of the literature was made. Although several authors (*1, 2, 12*) have studied the heat transfer characteristics of air in the Taylor system, there has been little work on fluids in general. In an attempt to generalize the heat transfer relations for fluids of various properties Haas and Nissan (*7*) presented heat transfer data for water and several glycerol-water solutions of different concentration. They found for the fluids they studied that

$$\frac{N_{Nu}}{N_{Nuk}} = \left(\frac{P}{P_c}\right)^m$$

where P is a form of Taylor number, and m depends on the fluid properties.

Ho, Nardacci, and Nissan (*10*) obtained an analytical relation which predicted the heat transfer characteristics of the Taylor vortex system for a small range of Taylor numbers above the critical value. However the theoretical analysis is only valid for air or for those fluids with a Prandtl number close to unity; it has the further restriction of narrow gap geometry and of ΔT being small.

The purpose of the present work is to extend the previous heat transfer results and to obtain a generalized empirical correlation for fluids of widely differing properties. In addition a more complete study of the temperature distribution in the annulus for various fluids is presented.

CALCULATIONS

It is convenient to introduce here some modifications in the definition of the Taylor number which were found useful in relating flows of different types to each other.

Brewster, Grosberg, and Nissan (3) have generalized the stability problems of concentric rotating cylinders by introducing a parameter P

$$P = \frac{\bar{v}\delta}{\nu}\sqrt{\frac{\delta}{r_1}} \tag{1}$$

where δ represents the region of instability which may or may not extend over the entire width of the gap and depends on R (the ratio of angular velocity of outer cylinder to the angular velocity of inner cylinder)

$$\frac{\delta}{d} \cong \frac{1}{1-R} \tag{2}$$

and v is the average velocity in the potentially unstable region only (of width δ).

For the case of stationary outer cylinder and narrow gaps, that is $d/r_m \to 0$, the following stability criterion may be established:

$$N_{Ta_c}{}^* = \frac{\Omega_{1c}{}^2 r_m d^3}{\nu^2} = 1{,}708 \qquad \left(\text{for } \frac{d}{r_m} \to 0,\ r_m \cong r_1\right) \tag{3}$$

$$P = \frac{1}{2}\frac{\Omega_1 r_1 d}{\nu}\sqrt{\frac{d}{r_1}} = \frac{1}{2}\sqrt{N_{Ta}{}^*} = \frac{1}{2}N_{Ta} \tag{4}$$

Kaye and Elgar (11) present a geometric factor F_g which corrects the point of instability for finite gap width:

$$P_c = 20.6\,F_g \quad \text{(for stationary outer cylinder)}$$

$$F_g = \frac{\pi^2}{41.2}\left(1-\frac{d}{2r_m}\right)^{-1} Z^{-1/2} \tag{5}$$

$$Z = 0.0571\left[1-0.652\left[\frac{\frac{d}{r_m}}{1-\frac{d}{2r_m}}\right]\right] +$$

$$0.00056\left[1-0.652\left[\frac{\frac{d}{r_m}}{1-\frac{d}{2r_m}}\right]\right]^{-1} \tag{6}$$

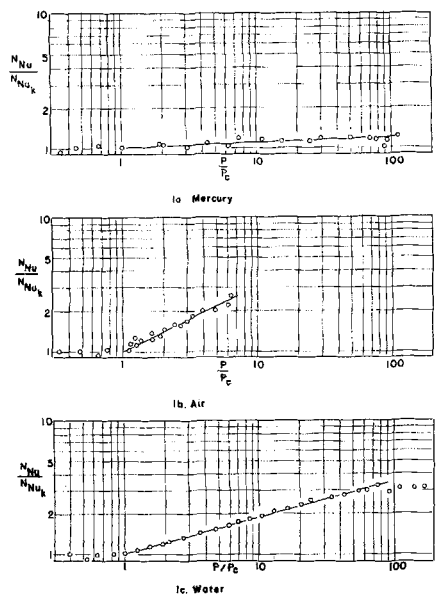

Fig. 1. Heat transfer results for mercury, air, water.

TABLE 1.

Fluid	ν, centistokes	N_{Pr}
Hg	0.08	0.025
H_2O	0.447	2.8
Air	22	0.7

For the purpose of calculation all the fluid properties are evaluated at the average temperature of the annulus:

$$\bar{T} = \frac{T_1 + T_2}{2} \tag{7}$$

The heat transfer coefficient is evaluated in the following way:

$$h = \frac{Q}{A_i(T_1 - T_2)} \tag{8}$$

Values of Q, A_i and T_1 and T_2 are directly measurable. Nusselt numbers may then be calculated from the expression

$$N_{Nu} = \frac{h(D_2 - D_1)}{k} = \frac{2\,h\,d}{k} \tag{9}$$

For pure conduction in the annulus the Nusselt number may be shown to be

$$N_{NuK} = \frac{2\frac{d}{r_1}}{\ln\left(\frac{d}{r_1}+1\right)} \tag{10}$$

where N_{NuK} refers to the Nusselt number for conduction. For $d/r_1 << 1$ Equation (10) reduces to $N_{NuK} = 2$.

POWER LAW OF HEAT TRANSFER FOR TAYLOR SYSTEM

In Part I an analytical derivation of the heat transfer relationship for the Taylor system restricted to fluids of $N_{Pr} = 1$ was attempted. A semiempirical power law of less rigor in derivation but of more widely applicable generality appears to have usefulness and will be derived and illustrated here.

Experimental Power Law

In the present work the heat transfer properties of mercury, water, and air in circumferential motion have been studied. Property values for these fluids are given in Table 1.

Heat transfer data were used to calculate values of the parameter P and Nusselt numbers as given by Equations (4) and (9). Values of $\frac{N_{Nu}}{N_{NuK}}$ vs. P/P_c were then plotted for each fluid (Figure 1).

In order to compare these data with those of other authors curves representing the available heat transfer data to date were plotted in Figure 2. The source of these data as well as property values are given in Table 2.

All the substances in Figure 2 can be seen to follow the functional relationship

$$\frac{N_{Nu}}{N_{NuK}} = \left(\frac{P}{P_c}\right)^m \tag{11}$$

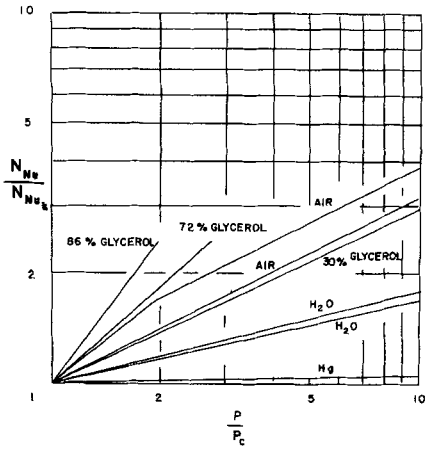

Fig. 2. Heat transfer results from present work and literature.

as given by Haas and Nissan (7).

Derivation of Power Law

$N_{Pr} = 1$. An interesting boundary-layer model for the Taylor vortex system has been proposed by Batchelor (4). As usual in such cases he has relegated the significance of the viscous forces to the layers of fluid near the cylinder surfaces. By considering the length of the boundary layer to be equal to the width of one vortex cell d, and by making a force balance between the centrifugal forces acting on the fluid throughout the boundary layer and the viscous forces, he has obtained relations for both the velocity at the outer edge of the boundary layer and the boundary-layer thickness itself. These relations may be written as

$$u_s \sim \Omega_1 (d r_1)^{1/2} \tag{12}$$

$$\frac{\delta_M}{d} \sim \frac{\nu^{1/2}}{\Omega_1^{1/2} r_1^{1/4} d^{3/4}} \tag{13}$$

Theoretical results based on this model and expressed in terms of torque showed very good agreement with torque data taken by Donnally and Simon (4).

In order to use the results of Batchelor's analysis for the heat transfer problem the following is noted. In boundary layer studies of heat transfer to flat layers [see Eckert and Drake (5) page 173] it is shown that

$$\frac{h}{k} \sim \frac{1}{\delta_T} \tag{14}$$

where δ_T refers to a thermal boundary-layer thickness. Multiplying relation (14) by d one gets

$$\frac{hd}{k} = N_{Nu} \sim \frac{d}{\delta_T} = \frac{1}{\delta_{T'}} \tag{15}$$

which is equivalent to stating that the heat transfer coefficient is inversely proportional to the thickness of the thermal boundary layer.

Relation (15) may be rewritten in terms of the momentum boundary-layer thickness as

$$N_{Nu} \sim \frac{1}{\delta_{T'}} = \frac{1}{p\delta'_m} \tag{16}$$

where

$$p = \frac{\delta_T}{\delta_m} \sim N_{Pr}^{-1/3} \tag{17}$$

for a flat plate. The Taylor number may be written as

$$N_{Ta} = \frac{\Omega_1 r_1^{1/2} d^{3/2}}{\nu} = \left[\frac{\Omega_1^{1/2} r_1^{1/4} d^{3/4}}{\nu^{1/2}}\right]^2 \tag{18}$$

Combining (13) and (18) one gets

$$(N_{Ta})^{-1} = \left(\frac{\delta_m}{d}\right)^2 = \delta_m'^2 \tag{19}$$

Combining (16), (17), and (19) one gets

$$N_{Nu} \sim N_{Pr}^{1/3} N_{Ta}^{1/2} \tag{20}$$

For $Pr = 1$

$$N_{Nu} \sim N_{Ta}^{1/2} \tag{21}$$

Relation (21) agrees with experimental heat transfer measurements for air ($N_{Pr} \simeq 1$), but for substances with

TABLE 2. COEFFICIENT m FOR VARIOUS FLUIDS

		ν(centistokes)	N_{Pr}	d, cm.	ΔT, °C.	β', 1/C°.	N_{Gr}	$\frac{N_{Pr}}{N_{Gr}}$	m
1.	Hg	0.08	0.025	0.34	8	18.17×10^{-5}	8.53×10^4	0.293×10^{-6}	0.07
2.	H_2O	0.88	6	1.20	14	20×10^{-5}	6.12×10^4	0.98×10^{-4}	0.23
3.	H_2O	0.88	6	1.80	12	20×10^{-5}	17.7×10^4	0.338×10^{-4}	0.21
4.	H_2O	0.447	2.8	0.34	15	28×10^{-5}	0.81×10^4	0.346×10^{-3}	0.25
5.	Air	20	0.7	2.0	25	27×10^{-4}	1.32×10^4	0.53×10^{-4}	0.5
6.	Air	20	0.7	1.2	25	27×10^{-4}	0.286×10^4	0.246×10^{-3}	0.5
7.	Air	20	0.7	0.4	25	27×10^{-4}	0.0106×10^4	0.66×10^{-2}	0.55
8.	Air	20	0.7	0.197	25	27×10^{-4}	0.00126×10^4	0.555×10^{-1}	0.6
9.	Air	20	0.7	0.2	25	27×10^{-4}	0.00132×10^4	0.53×10^{-1}	0.6
10.	Air	16	0.7	0.155	28	27×10^{-4}	0.00108×10^4	0.593×10^{-1}	0.7
11.	Air	16	0.7	0.242	28	27×10^{-4}	0.0041×10^4	0.171×10^{-1}	0.67
12.	Air	16	0.7	0.368	28	27×10^{-4}	0.00144×10^4	0.486×10^{-2}	0.65
13.	Air	16	0.7	0.700	28	27×10^{-4}	0.099×10^4	0.71×10^{-3}	0.5
14.	Air	22	0.7	0.34	30	27×10^{-4}	0.00474×10^4	0.148×10^{-1}	0.5
15.	30% glycerol	2.05	16.5	1.20	14	29.9×10^{-5}	1.7×10^4	0.97×10^{-3}	0.48
16.	30% glycerol	2.05	16.5	1.80	8	29.9×10^{-5}	3.24×10^4	0.510×10^{-3}	0.50
17.	72% glycerol	18	180	1.20	17	43.7×10^{-5}	0.039×10^4	0.461	0.889
18.	86% glycerol	75	750	1.20	18	48.4×10^{-5}	0.00261×10^4	28.7	1.31

(1), (4), (14)—Ho (1962).
(2), (3), (15), (16), (17), (18)—Haas and Nissan (1961 b).
(5), (6), (7), (8), (9)—Tachibana et al. (1960).
(10), (11), (12), (13)—Bjorklund and Kays (1959).
$N_{Gr} = g\Delta T\beta' d^3/\gamma^2$ = Grashoff number.
g = 980 cm./sec.^{2} = gravitational acceleration.

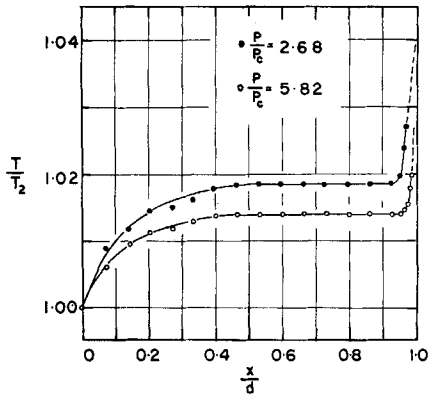

Fig. 3a. Radial temperature profiles for 50% glycerine-water solution.

$N_{Pr} \neq 1$ expression (20) does not fit the data. The agreement of theory and experiment for air is most probably due to the similarity of the thermal and momentum boundary-layer thickness for $N_{Pr} = 1$. However for substances with Prandtl numbers different from 1, the simple flat-plate analysis is not adequate enough to represent the interaction between the thermal and momentum vortex boundary layers.

$N_{Pr} \neq 1$. The power law for fluids with $N_{Pr} \neq 1$ may be obtained from radial temperature profile measurements in the annulus between the cylinders. The shape of a radial temperature profile ($R = 0$) in the Taylor system has been obtained by several authors (*8, 9, 12*). It consists of regions of sharp temperature gradient near the walls of the cylinders which enclose a region of very small temperature gradient. From papers by Haas and Nissan (*8*) and Ho (*9*) it was noted that the thickness of the region of sharp temperature gradient seemed to be a function of the fluid in the annulus and the speed of rotation. It was therefore decided to obtain a series of profiles for fluids of varying properties and at various speeds of rotation.

Figure 3*a* shows two profiles for a 50% glycerine-water solution taken at different speeds of rotation (corresponding to 2.68 P/P_c and 5.82 P/P_c). The ordinate represents a ratio of the temperature at a position in the annulus (T) to that at the wall of the outer cylinder (T_2); the abscissa is a dimensionless annulus thickness based on the gap diameter d.

In order to obtain the thickness of the region of sharp temperature gradient the flat center portion of each curve was extrapolated at each end. The distance between the wall and the point where the temperature curve breaks away from the extrapolated center line is the dimensionless thickness of the region of sharp temperature gradient, δ_T'.

From the profiles in Figure 3*a* it can be seen that δ_T' decreases with increasing speed (P/P_c).

Figure 3*b* shows temperature profiles for water and a 50% glycerine-water solution at approximately the same P/P_c. It can be seen that the water has a thicker δ_T'.

In order to compare the data for all the fluids studied (temperature profiles were taken for water and 30, 50, and 72% glycerine-water solution) values of δ_T' vs. P/P_c were plotted in Figure 4 for each fluid. As can be seen from Figure 4*a* the experimental points vary in such a manner that straight lines drawn through them should fit a relationship of the form

$$\delta_T' \sim \left(\frac{P}{P_c}\right)^{-e} \tag{22}$$

where e is a function of the fluid properties.

If now the thickness of the region of sharp temperature gradient as given by relation (22) is considered as a thermal boundary-layer thickness, and relation (15) is again assumed to be valid, then combination of (15) and (22) gives

$$N_{Nu} \sim \left(\frac{P}{P_c}\right)^{e} \tag{23}$$

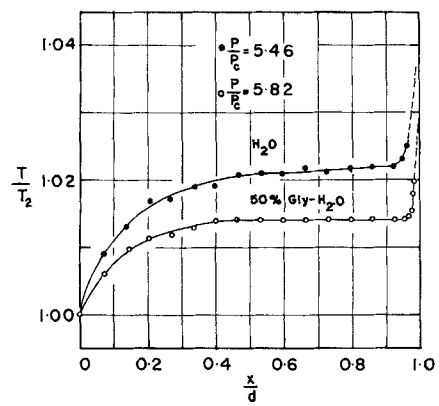

Fig. 3b. Radial temperature profiles for water and a 50% water-glycerine solution.

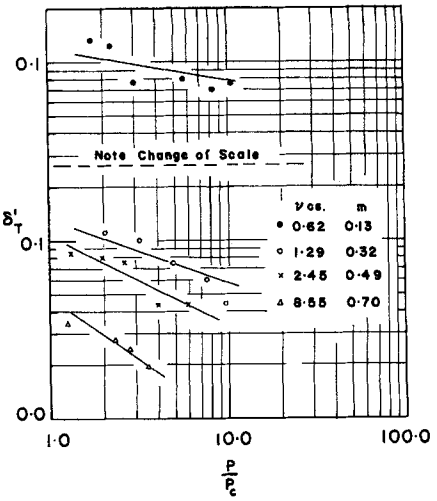

Fig. 4a. Thermal boundary layer thickness for various fluids—inner cylinder.

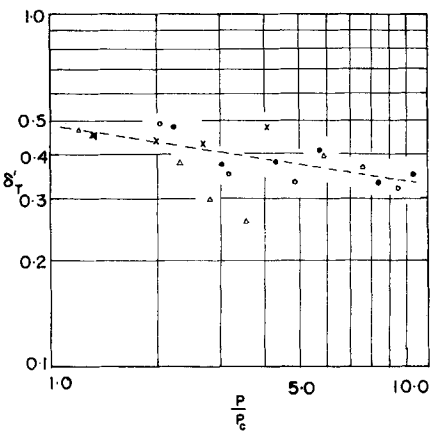

Fig. 4b. Thermal boundary layer thickness for various fluids—outer cylinder.

As was mentioned earlier Haas and Nissan (7) have found that

$$N_{Nu} \sim \left(\frac{P}{P_c}\right)^m \tag{24}$$

and have obtained values of m for several fluids.

Relations (23) and (24) are identical except for the exponents. From Figure 32 in Haas (6) values of m were obtained for the fluids used in this experiment. On the assumption that $m = e$ the lines seen in Figure 4*a* were plotted through the use of relation (22). These lines can be seen to give a reasonable fit to the experimental points obtained from the temperature profile measurements; therefore the assumption of $m = e$ would seem to be a good one which makes (23) and (24) identical.

Based on the above analysis it seems logical that what has been previously called the region of sharp temperature gradient may in fact be treated as a thermal boundary-layer thickness.

Although the above analysis is based on relatively few data points, it is believed that the relation $h/k \sim 1/\delta_T'$ is basically correct for the Taylor system and that further study in this area may be fruitful in determining the exact mechanism of heat transfer in the Taylor system.

Figure 4*b* is a plot of δ_T' vs. P/P_c for the outer cylinder surface. The points show considerably more scatter than those in Figure 4*a*. This scatter is probably due to the more gradual change in slope of the temperature profiles near the outer cylinder which makes it difficult to obtain the exact width of the outer boundary-layer thickness. These points do however exhibit a characteristic negative slope which would be expected in view of the preceding analysis.

EXPERIMENTAL DETERMINATION OF THE EXPONENT M

The data obtained in the present study were combined with those of other authors in order to obtain a general expression for m. Values of N_{Pr}/N_{Gr} were obtained for each fluid and plotted against the corresponding value of m as given in Table 2 (Figure 5). The points in Figure 5 are represented by the expression

$$m = \left(\frac{N_{Pr}}{N_{Gr}}\right)^{1/6} \tag{25}$$

with $1 < P/P_c < 100$ and $10^{-7} < N_{Pr}/N_{Gr} < 40$

Thus Equation (11) in conjunction with (25) gives the heat transfer coefficients for the Taylor system for a wide range of property values and speeds of rotation.

CONCLUSIONS

The heat transfer relation for the Taylor vortex system

$$\frac{N_{Nu}}{N_{Nuk}} = \left(\frac{P}{P_c}\right)^m$$

is corroborated by both temperature profile and heat transfer measurements. The exponent m is experimentally found to follow the equation

$$m = \left(\frac{N_{Pr}}{N_{Gr}}\right)^{1/6}$$

where $10^{-7} < N_{Pr}/N_{Gr} < 40$ and $1 < P/P_c < 100$.

ACKNOWLEDGMENT

Grateful thanks are due to the National Science Foundation for the financial support of this work through their Grant G-11356 made to A. H. Nissan.

NOTATION

A = constant in Equation (4), Part I
A_i = surface area of inner cylinder
a_c = equilibrium amplitude
B = constant in Equation (4), Part I
C = constant in Equation (4), Part I
C^1 = constant in Equation (9), Part I
D = constant in Equation (4), Part I
D^1 = constant in Equation (10), Part I
D_1 = diameter of inner cylinder
D_2 = diameter of outer cylinder
d = width of annulus
e = constant in Equation (22), Part II
Fg = correction factor for finite gap widths
g = gravitational acceleration
h = heat transfer coefficient
K = thermal diffusivity
k = thermal conductivity
m = constant in Equation (11), Part II
N_{Nu} = Nusselt number
N_{Nuk} = Nusselt number for pure conduction
N_{Pc} = Peclet number
N_{Pr} = Prandtl number
N_{Gr} = Grashoff number
P = generalized stability parameter
P_c = critical generalized stability parameter
p = δ_T/δ_M
Q = total heat transfer rate
q = heat transfer rate

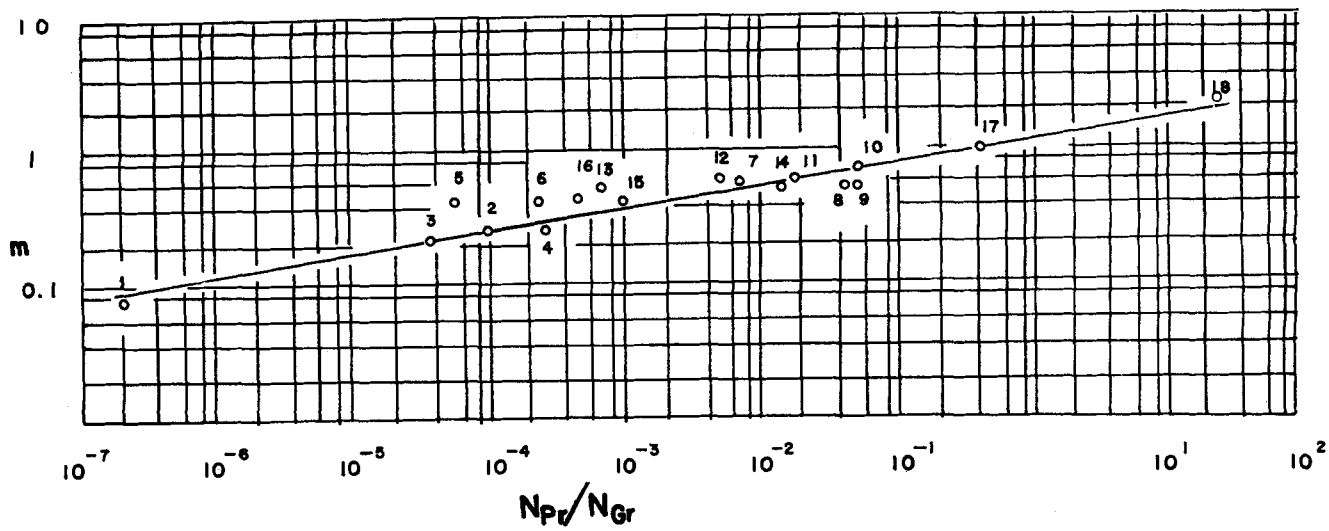

Fig. 5. Coefficient m vs. N_{PR}/N_{Gr}.

q_1,q_2,q_1,q_2 = General quantities given by Equation (5), Part I
R = ratio of cylinder speeds
r = radius or coordinate
r_1 = radius of inner cylinder
r_2 = radius of outer cylinder
r_m = mean radius
S = shape function given by Equation (23), Part I
T = temperature
$\overline{T}$ = average temperature in annulus
T_1 = temperature of inner cylinder
T_2 = temperature of outer cylinder
N_{Ta^*} = Taylor number
N_{Ta} = Taylor number $(\sqrt{N_{Ta^*}})$
N_{Tac^*} = critical Taylor number
N_{Tac} = critical Taylor number $(\sqrt{N_{Tac^*}})$
t = time
t_1 = first harmonic component of temperature disturbance
u = velocity in r direction
u_1 = first harmonic component of u disturbance
u_s = velocity at edge of boundary layer
v = velocity in θ direction.
v_1 = first harmonic component of v disturbance
$\overline{v}$ = average velocity of flow in potentially unstable region of annulus
w = velocity in z direction
w_1 = first harmonic component of w disturbance
Z = constant given by Equation (22), Part I
z = coordinate

Greek Letters

α = dimensionless constant
β = constant in Equation (11), Part I
β^1 = coefficient of volume expansion
δ = potentially unstable region of gap
δ_M = momentum boundary-layer thickness
$\delta_{M'}$ = δ_M/d
δ_T = thermal boundary-layer thickness
δ_{T^1} = δ_T/d
ν = kinematic viscosity
τ = dimensionless coordinate
θ = coordinate
λ = dimensionless wave length
σ = dimensionless constant given in Equation (13), Part I
Ω = speed of rotation of cylinder (rad./sec.)
Ω_1 = rotational speed of inner cylinder
Ω_2 = rotational speed of outer cylinder

LITERATURE CITED

1. Becker, K. M., and J. Kaye, *Am. Soc. Mech. Engrs. Paper No. 61-SA-19* (1961).
2. Bjorklund, I. S., and W. M. Kays, *Am. Soc. Mech. Engrs. Heat Transfer Journal*, **81**, 175 (1959).
3. Brewster, D. B., P. Grosberg, and A. H. Nissan, *Proc. Roy. Soc.*, **A251**, 76 (1959).
4. Donnelly, R. J., and N. J. Simon, *J. Fluid. Mech.*, 7, 401 (1960).
5. Eckert, E. R. G., and R. M. Drake, "Heat and Mass Transfer," McGraw-Hill, New York (1959).
6. Haas, F. C., Ph.D. thesis, Rensselaer Polytechnic Institute, Troy, New York (1960).
7. ———, and A. H. Nissan, International Heat Transfer Conference, Boulder, Colorado, Vol. 3, 643 (1961).
8. ————————, *Proc. Roy. Soc.*, **A261**, 215 (1961).
9. Ho, C. Y., Ph.D. thesis, Rensselaer Polytechnic Institute, Troy, New York (1962).
10. ———, J. L. Nardacci, and A. H. Nissan, *A.I.Ch.E. Journal*, **10**, p. 194 (1964).
11. Kaye, J., and E. C. Elgar, *Trans. Am. Soc. Mech. Engrs.*, **80**, 753 (1958).
12. Tachibana, F., S. Fukui, and H. Mitsumura, *J. Soc. Mech. Engrs.*, **3**, No. 9, p. 119 (1960).

Manuscript received March 12, 1963; revision received August 2, 1963; paper accepted August 5, 1963.

Hydrates at High Pressures: Part I. Methane-Water, Argon-Water, and Nitrogen-Water Systems

DONALD R. MARSHALL, SHOZABURO SAITO, and RIKI KOBAYASHI

William Marsh Rice University, Houston, Texas

A gas hydrate may be defined as the stable crystalline icelike complex formed from the lower molecular weight nonpolar and slightly polar compounds and water when a mixture of these is subjected to external pressure. Gas hydrates may occur above and below the ice point and fall in a subdivision of the class of compounds known as *inclusion compounds.*

The first hydrate of this type, chlorine hydrate, was discovered by Davy in 1810. After this discovery considerable work was done by Villard (*17*) and De Forcrand (*9, 10*) on the direct determination of hydrate formulas and formation conditions.

Donald R. Marshall is with E. I. du Pont de Nemours and Company, Orange, Texas.